D0904990

VENDOR DESIGN ANALYSIS REVIEW

☑ Approved - No Comments / No Impact on COLR Values

☐ Approved - No Comments / Impact on COLR Values / NS&L Review Required

Approval of this design analysis does not relieve supplier from full compliance with contract or purchase order requirements.

Approved By _____ Date 6/29/01

NS&L Review By N/A Date _____

ROCHESTER GAS & ELECTRIC CORP.
ROCHESTER, NY

Report No.: SIR-99-036
Revision No.: 0
Project No.: RGE-09Q
File No.: RGE-09Q-401
June 1999

Leak-Before-Break Evaluation of Portions of the Accumulator A and B Piping at R. E. Ginna Nuclear Power Station

Prepared for:

Rochester Gas & Electric Corporation

Prepared by:

Structural Integrity Associates, Inc.
San Jose, California

Prepared by: _____ Date: 6/10/99
G. A. Miessi

Prepared by: _____ Date: 6-10-99
R. L. Bax

Reviewed and Approved by: _____ Date: 6/10/99
N. G. Cofie

REVISION CONTROL SHEET

Document Number: SIR-99-036

Title: Leak-Before-Break Evaluation of Portions of the Accumulator A and B Piping at R. E. Ginna Nuclear Power Station

Client: Rochester Gas & Electric Corporation

SI Project Number: RGE-09Q

Section	Pages	Revision	Date	Comments
-	-	A	04/09/99	Draft Issue
-	-	0	06/10/99	Initial Issue

EXECUTIVE SUMMARY

The high energy portions of the Safety Injection Accumulator A and B piping at R. E. Ginna Nuclear Power Station (Ginna) were evaluated for leak-before-break (LBB) behavior in accordance with the 10 CFR 50, Appendix A GDC-4 and NUREG-1061, Vol. 3. The piping considered in this evaluation is adjacent to the cold legs of the reactor coolant system (RCS). They are 10-inch Schedule 160 piping, fabricated from Type 316 stainless steel. The operating pressure for the accumulator piping is 2250 psia and the operating temperature is 550°F.

The evaluation consisted of determining critical flaw sizes and leakage flaw sizes at weld locations on the affected piping using stresses at each location. The critical flaw sizes were calculated using the elastic-plastic fracture mechanics (EPFM) J-Integral/Tearing Modulus (J/T) approach and conservative generic material properties. The detectable leakage at Ginna is 0.25 gpm. Based on the required margin of 10 on leakage in NUREG-1061, Vol. 3, the critical flaw sizes must be greater than the crack size which producers 2.5 gpm leakage to assure leak-before-break. Critical flaw sizes were determined for normal + SSE loads and were shown to be at least two times the length of the 2.5 gpm leakage flaws. Critical flaw sizes were determined with a factor of $\sqrt{2}$ on normal + SSE loads and were shown to have lengths greater than the 2.5 gpm leakage flaws. A fatigue crack growth analysis was also performed which showed that the growth of postulated semi-elliptical, inside surface flaws with an initial size slightly in excess of ASME Section XI acceptance standards was not significant.

The following provides a summary of the LBB evaluation summarized along the lines of the "Recommendations for Application of the LBB Approach" in the NUREG-1061 Vol. 3 executive summary:

(a) The accumulator piping at Ginna is constructed of very ductile stainless steel that is not susceptible to cleavage-type fracture. In addition, it has been shown to be not susceptible to the effects of corrosion, high cycle fatigue or water hammer.

(b) Loadings have been determined from the original piping analysis, and were due to pressure, dead weight, thermal expansion and seismic. All stress locations in the affected portion of the piping model were considered.

(c) Plant-unique material properties were not available. Lower-bound generic industry data for the piping and welds were conservatively used in the evaluations.

(d) Crack growth analysis was conducted at the critical location, considering the cyclic stresses predicted to occur over the life of the plant. For a crack in the stainless steel materials, an initial crack with depth of 15% of the wall was predicted to grow to 16% of wall. Given that the controlling location is inspected in accordance with ASME Section XI requirements in each 10-year interval, this growth is not considered to be significant. It was also demonstrated that the crack had more of a propensity to grow in the radial direction than in the circumferential direction, demonstrating that it would exhibit leak-before-break behavior.

(e) The detectable leakage at Ginna is 0.25 gpm. Based on the required margin of 10 on leakage, the leakage flaw size has been taken as the flaw size predicted to produce 2.5 gpm leakage.

(f) The accumulator piping subject to this evaluation is less than 10 feet in length and is not geometrically complex. In addition, there is no flow in the lines during normal operation, including no possibility of cold in-leakage past the isolation valves, such that complex system transients are not involved. Thus, no system evaluation was conducted.

(g) It was shown for the controlling location that crack growth of a leakage size crack for 10 SSE seismic cycles would grow the crack by no more than 1% of the leakage flaw size. This is not significant compared to the margin between the leakage-size crack size and the critical crack size.

(h) For all locations, the critical size circumferential crack was determined for the combination of normal plus safe shutdown earthquake (SSE) loads. The 2.5 gpm leakage size crack was shown to have a length that was at least a factor of two less than the critical crack size. Axial cracks were not considered since these always exhibit higher leakage than circumferentially-oriented cracks.

(i) For all locations, the critical crack size was determined for the combination of $\sqrt{2}$ times the normal plus SSE stresses. The 2.5 gpm leakage size crack was shown to be less than the critical crack size (2a). In no case was the limiting critical flaw size governed by this criterion.

(j-n) No testing was conducted to determine material properties. Instead, generic lower bound piping material toughness and tensile properties were used in the evaluations. The material properties so determined have been shown to be applicable near the upper range of normal plant operation and exhibit ductile behavior at these temperatures. This data is widely accepted by industry for conducting J-T fracture mechanics analysis and has been used by the U.S. NRC in a previous safety evaluation of the RHR system at Ginna with similar material.

(o) Limit-load analysis was not utilized in this evaluation.

Thus, it is concluded that the high energy portions of the accumulator piping evaluated in the report qualifies for the application of leak-before-break analysis to demonstrate that it is very unlikely that the piping could experience an unforeseen large pipe break.

Table of Contents

List of Tables

List of Figures

1.0 INTRODUCTION

1.1 Background

This report documents evaluations performed by Structural Integrity Associates (SI) to determine the leak-before-break (LBB) capabilities of portions of the Safety Injection Accumulator A and B piping at the R. E. Ginna Nuclear Power Station (Ginna). These evaluations were undertaken to address high energy line break concerns at these locations.

The Class 1 portion of the Accumulator A piping considered is shown in Figure 1-1. It extends from the reactor coolant cold leg and between check valve 867A and motor operated valve (MOV) 721 (Nodes 960 through 856) in Figure 1-1 [1a, 1b]. This portion of the Accumulator A piping also serves as part of the residual heat removal (RHR) system. All the nodal stress locations on the affected portion with the exception of Node 856 were considered in the LBB evaluation of portions of the RHR line which has been accepted by the NRC [2,3,4]. As such, only Node 856 will be included in the present evaluation for the Accumulator A piping. The Accumulator B piping is shown in Figure 1-2. The affected portion extends from the connection to the cold leg (Node 60) up to MOV 867B (Node 80) [1c]. Only these two nodes are considered for the Accumulator B piping in this evaluation. The Accumulator A and B lines are 10 inch, Schedule 160 piping and are fabricated from Type 316 stainless steel.

1.2 Leak-Before-Break Methodology

NRC SECY-87-213 [5] covers a final broad scope rule to modify General Design Criterion 4 (GDC-4) of Appendix A, 10 CFR Part 50. This amendment to GDC-4 allows exclusion from the design basis of dynamic effects associated with high energy pipe rupture by application of LBB technology.

Definition of the LBB approach and criteria for its use are provided in NUREG-1061 [6]. Volume 3 of NUREG-1061 defines LBB as "...the application of fracture mechanics technology to demonstrate that high energy fluid piping is very unlikely to experience double-ended ruptures or their equivalent as longitudinal or diagonal splits." The particular crack types of interest include

circumferential through-wall cracks (TWC) and part-through-wall cracks (PTWC), as well as axial or longitudinal through-wall cracks (TWC), as shown in Figure 1-3.

LBB is based on a combination of in-service inspection (ISI) and leak detection to detect cracks, coupled with fracture mechanics analysis to show that pipe rupture will not occur for cracks smaller than those detectable by these methods. A discussion of the criteria for application of LBB is presented in Section 2 of this report, which summarizes the NUREG-1061 requirements.

The approach to LBB which has gained acceptance for demonstrating protection against high energy line break (HELB) in safety-related nuclear piping systems is schematically illustrated in Figure 1-4. Essential elements of this technique include critical flaw size evaluation, crack propagation analysis, volumetric nondestructive examination (NDE) for flaw detection/sizing, leak detection, and service experience. In Figure 1-4, a limiting circumferential crack is modeled as having both a short through-wall component, and an axisymmetric part-through-wall crack component. Leak detection establishes an upper bound for the through-wall crack component while volumetric ISI limits the size of undetected part-through-wall defects. These detection methods complement each other, since volumetric ISI techniques are well suited to the detection of long cracks while leakage monitoring is effective in detecting short through-wall cracks. The level of ISI required to support LBB involves volumetric inspection at intervals determined by fracture mechanics crack growth analysis, which would preclude the growth of detectable part-through-wall cracks to a critical size during an inspection interval. The objective of this fatigue evaluation is to limit potentially undetected defect sizes to those which would be allowed under ASME Section XI rules. For through-wall defects, crack opening areas and resultant leak rates are compared with leak detection limits.

The net effect of complementary leak detection and ISI is shown by the shaded region of Figure 1-4 as the largest undetected defect that can exist in the piping at any given time. Critical flaw size evaluation, based on elastic-plastic fracture mechanics techniques, is used to determine the length and depth of defects that would be predicted to cause pipe rupture under specific design basis loading conditions, including abnormal conditions such as a seismic event and including appropriate safety margins for each loading condition. Crack propagation analysis is used to determine the time

interval in which the largest undetected crack could grow to a size which would impact plant safety margins. A summary of the elements for a leak-before-break analysis is shown in Figure 1-5. Service experience, where available, is useful to confirm analytical predictions as well as to verify that such cracking tends to develop into "leak" as opposed to "break" geometries.

In accordance with NUREG-1061, Volume 3 [6] and other NRC guidance on the topic, the leak-before-break technique for high energy piping systems in a nuclear power plant should include the following considerations.

- Elastic-plastic fracture mechanics analysis of load carrying capacity of cracked pipes under worst case normal loading, with safe-shutdown earthquake (SSE) loads included. Such analysis should include recent elastic-plastic fracture data applicable to pipe weldments and weld heat affected zones where appropriate.

- Consideration of pipes under limit load conditions for the piping system, as applicable.

- Linear elastic fracture mechanics analysis of subcritical crack propagation to determine ISI (in-service inspection) intervals for long, part-through-wall cracks.

Piping stresses have a dual role in LBB evaluations. On one hand, higher maximum (design basis) stresses tend to yield lower critical flaw sizes, which result in smaller flaws for leakage and a lower leakage rate. On the other hand, higher operating stresses tend to open cracks more for a given crack size and create a higher leakage rate. Because of this duality, the use of a single maximum stress location for a piping system may result in a non-conservative LBB evaluation. This LBB evaluation will, therefore, be performed in such a manner that the affected nodal locations for the piping models of the accumulator piping will be specifically addressed.

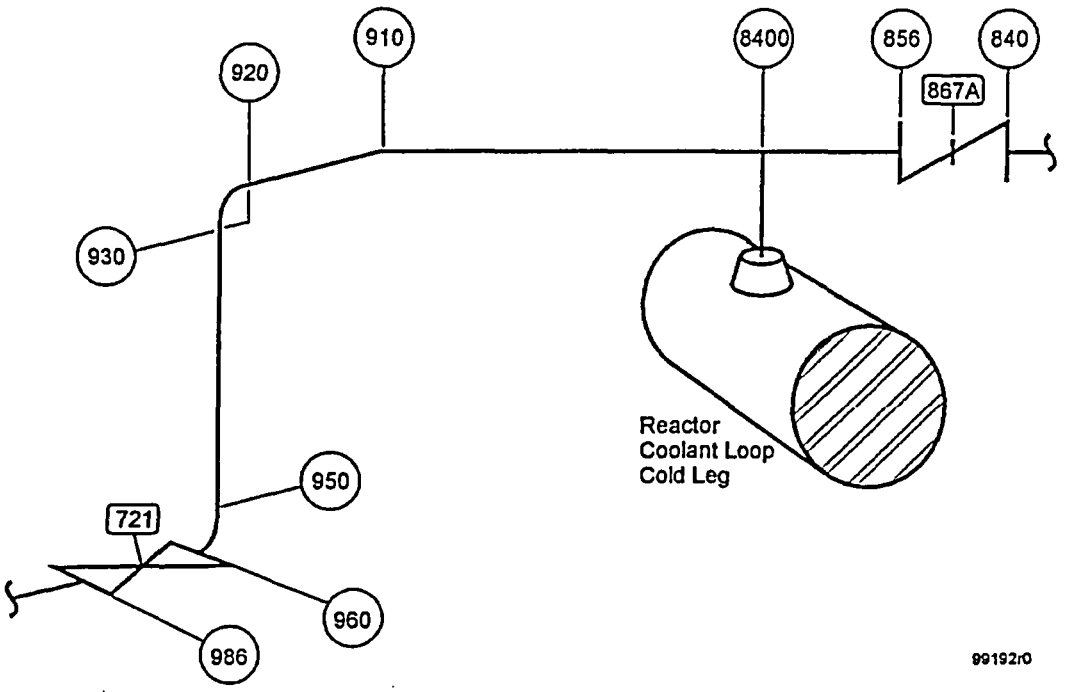

Figure 1-1. Schematic of Accumulator A Piping Adjacent to the Cold Leg

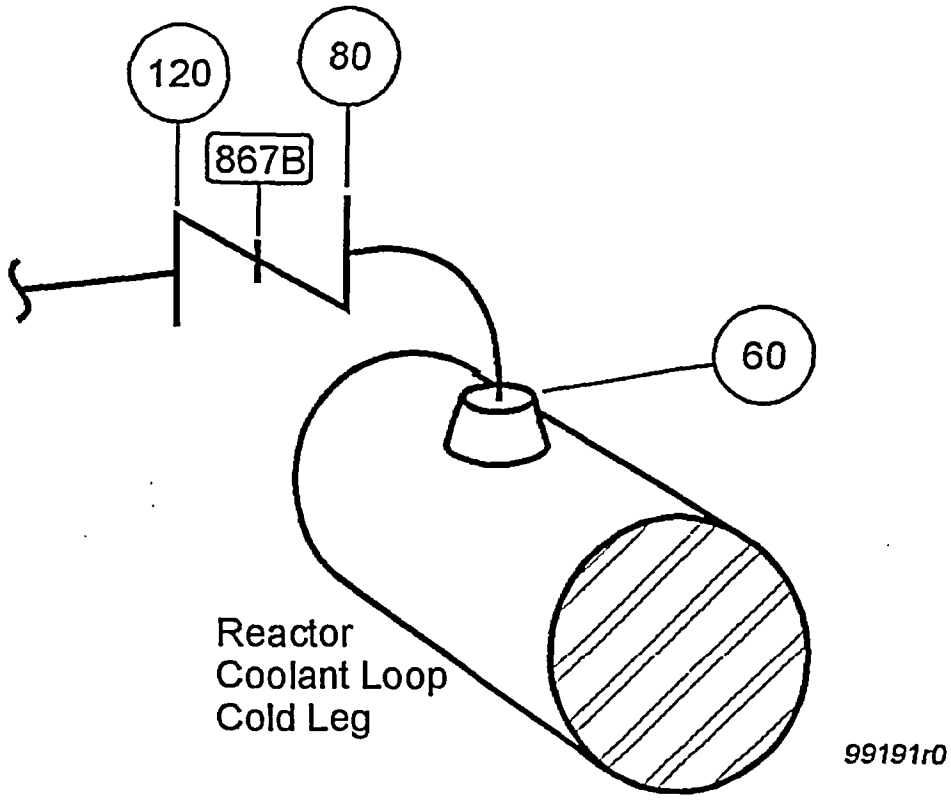

Figure 1-2. Schematic of Accumulator B Piping Adjacent to the Cold Leg

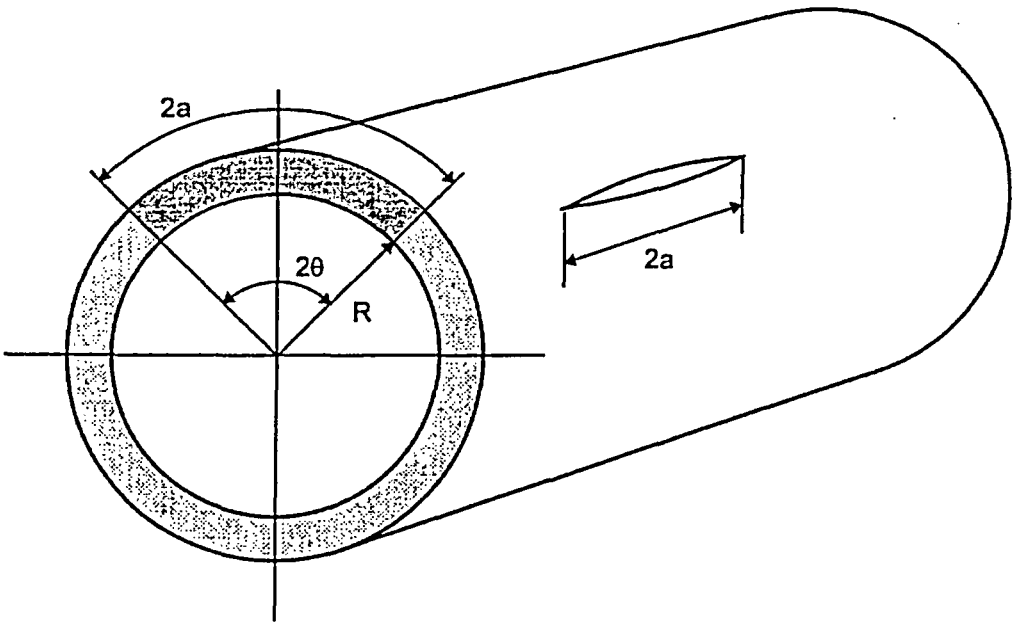

a. Circumferential and Longitudinal Through-Wall Cracks of Length 2a.

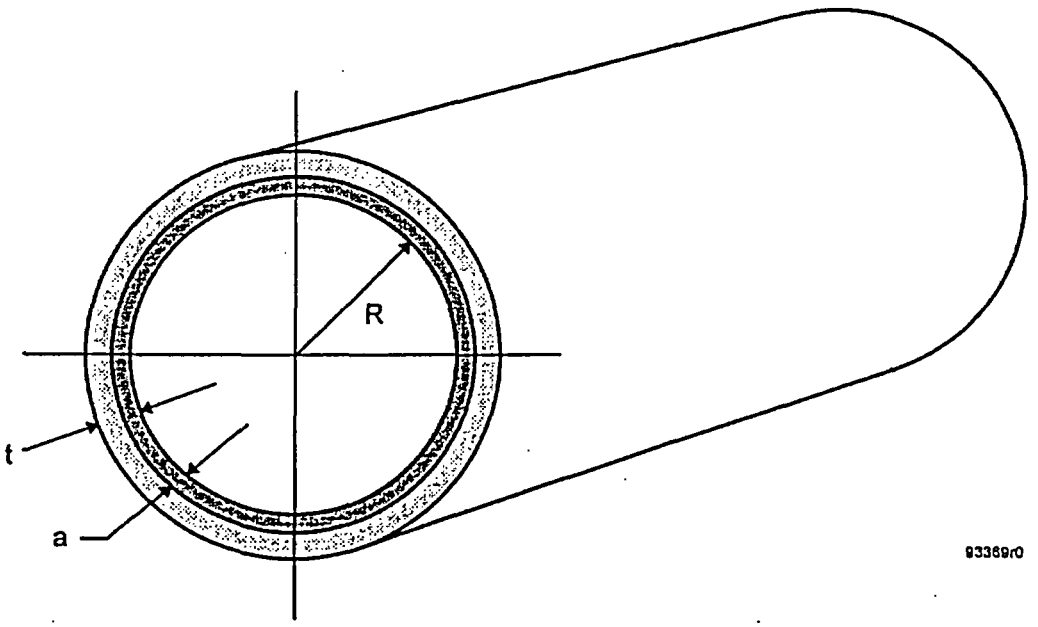

b. Circumferential 360 Part-Through-Wall Crack of Depth a.

Figure 1-3. Representation of Postulated Cracks in Pipes for Fracture Mechanics Leak-Before-Break Analysis

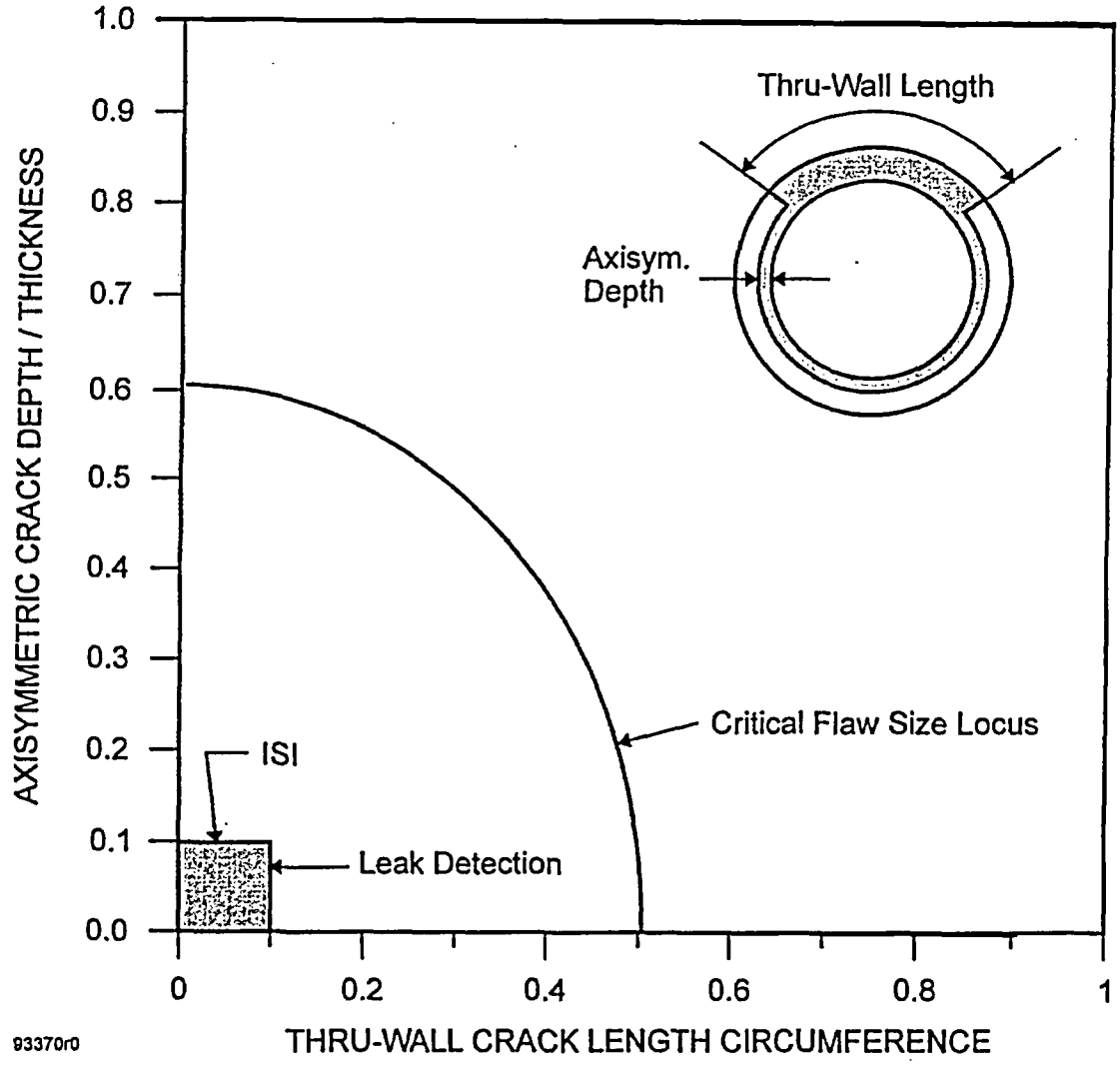

Figure 1-4 Illustration of ISI (UT)/Leak Detection Approach to Protection Against Pipe Rupture

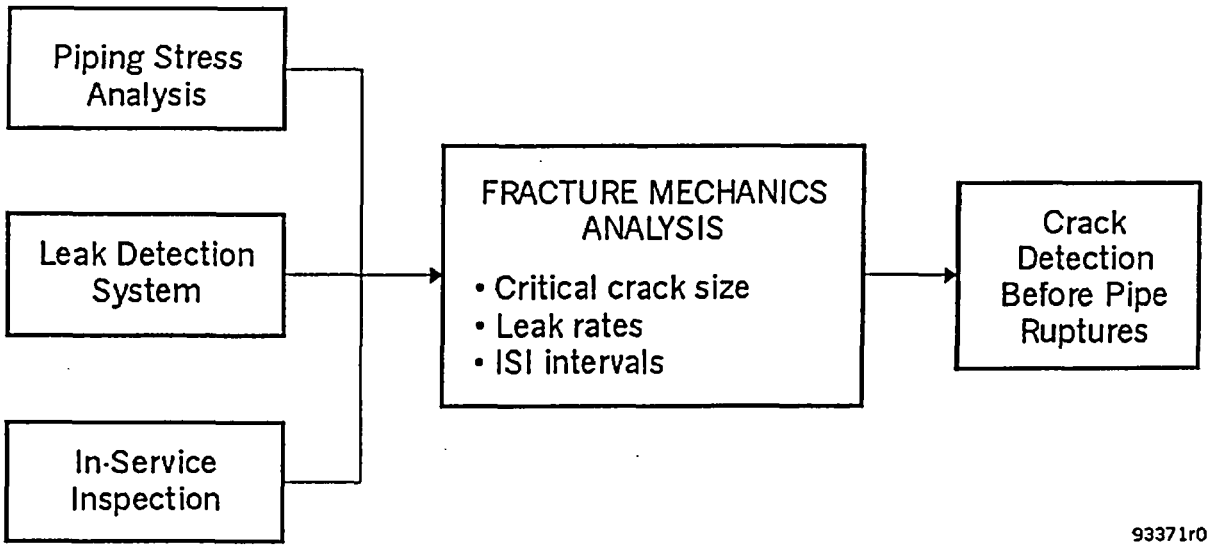

Figure 1-5. Leak-Before-Break Approach Based on Fracture Mechanics Analysis with In-service Inspection and Leak Detection

2.0 CRITERIA FOR APPLICATION OF LEAK-BEFORE-BREAK APPROACH

NUREG-1061, Volume 3 [6] and GDC-4 (SRP 3.6.3) [5] identify several criteria to be considered in determining applicability of the leak-before-break approach to piping systems.

Section 5.2 of Reference 3 provides an extensive discussion of the criteria for performing leak-before-break analyses. The details of that discussion will not be repeated here, but a summary of various requirements as applied to evaluation of the accumulator piping at Ginna is provided below.

2.1 Criteria for Through-Wall Flaws

Acceptance criteria for critical stresses and critical flaws are:

1. The flaw which is required to produce an "acceptable leakage rate" is smaller than the critical flaw length associated with the maximum stress (with SSE) by a factor of 2.

2. The stress required to make the "acceptable leakage rate" flaw critical is greater than the maximum stress (with SSE) by a factor of at least $\sqrt{2}$.

3. The net section collapse criterion (NSCC) approach may be used to compute the critical flaw size provided a safety factor of 3 is placed on normal service stresses.

It has been found in previous LBB evaluations conducted by Structural Integrity Associates (SI), that in general, the first criterion bounds the second. However, in this evaluation, both criteria will be considered for completeness. The elastic-plastic fracture mechanics (EPFM) approach is generally conservative relative to the NSCC approach when applied to ferritic piping. Therefore, only EPFM principles will be applied in this evaluation.

2.2 Criteria for Part-Through-Wall Flaws

NUREG-1061, Volume 3 [6] requires demonstration that a long part-through-wall flaw which is detectable by ultrasonic means will not grow due to fatigue to a depth which would produce

instability over the life of the plant. This is demonstrated in Section 6.0 of this report, where the analysis of subcritical crack growth is discussed.

2.3 Other Mechanisms

NUREG-1061, Volume 3 [6] and GDC-4 [5] limit applicability of the leak-before-break approach to those locations where degradation or failure by mechanisms such as water hammer, erosion/corrosion, fatigue, and intergranular stress corrosion cracking (IGSCC) is not a significant possibility. These mechanisms were considered for the accumulator piping at Ginna, as reported in Section 3 of this report.

3.0 CONSIDERATION OF WATER HAMMER, CORROSION AND FATIGUE

NUREG-1061, Volume 3 [6] and GDC-4 [5] state that LBB should not be applied to high energy lines susceptible to failure from the effects of water hammer, corrosion or fatigue. These potential failure mechanisms are thus discussed below with regard to the accumulator piping at Ginna, and it is concluded that the above failure mechanisms do not invalidate the use of LBB for this piping system.

3.1 Water Hammer

A comprehensive study performed in NUREG-0927 [7] indicated that the probability of water hammer occurrence in the affected portions of the accumulator system of a PWR is very low. In addition, RG&E has utilized EPRI guidelines and research results (References 8 and 9) to prevent, mitigate or accommodate water hammer events in Ginna systems.

3.2 Corrosion

Two corrosion damage mechanisms which can lead to rapid piping failure are intergranular stress corrosion cracking (IGSCC) in austenitic stainless steel pipes and flow-assisted corrosion (FAC) in carbon steel pipes. IGSCC has principally been an issue in austenitic stainless steel piping in BWRs [10] resulting from a combination of tensile stresses, susceptible material and oxygenated environment. IGSCC is not typically a problem for the primary loop of a PWR such as the Accumulator piping under consideration since the environment has relatively low concentrations of oxygen.

Erosion-corrosion is not anticipated to be a problem for this system since it is fabricated from stainless steel piping which is not susceptible to erosion-corrosion [11].

3.3 Fatigue

Known fatigue loadings and the resultant possible crack growth have been considered by the analyses reported in Section 6.0 of this report. Based on these results, it is concluded that fatigue will not be a significant issue for the accumulator piping at Ginna.

4.0 PIPING MATERIALS AND STRESSES

4.1 Piping System Description

The mathematical models for the Accumulator A and B piping system at Ginna is shown in Figures 1-1 and 1-2. The piping is fabricated from SA-376 Type 316 stainless steel. The welds are fabricated using the shielded metal arc welding (SMAW) processes [12]. The lines are fabricated from 10-inch schedule 160 piping. The operating pressure for the RHR lines is 2235 psig and the operating temperature is 550° [13].

4.2 Material Properties

The material for the accumulator piping is Type 316 stainless steel. All the stainless steel welds are fabricated using stainless steel weld metal with shielded metal are welding (SMAW). NUREG-1061, Vol. 3 recommends that actual plant specific material properties including stress-strain curves and J-R material properties be used in the LBB evaluations. Actual archival materials for the accumulator piping is not available. Hence, in lieu of this requirement, material properties associated with the least favorable material and welding processes from industry wide generic material sources will be used to provide a conservative assessment of critical flaw sizes and leakage flaw sizes.

The material properties of interest for fracture mechanics and leakage calculations are the Modulus of Elasticity (E), the yield stress (S_y), the ultimate stress (S_u), the Ramberg-Osgood parameters for describing the stress strain curve (α and n), the fracture toughness (J_{IC}) and power law coefficient for describing the material J Resistance curve (C and N).

In determining the material properties to use in the LBB evaluation, the less favorable of the base metal and weld metal properties are selected for use in the evaluation. Because of its very low toughness and susceptibility to thermal aging, the SMAW weld properties are expected to provide the most conservative critical flaw and leakage flaw sizes. The conservative stress-strain properties for the SMAW weldments at 550°F in Reference 14 which formed the basis for the flaw acceptance criteria in ASME Section XI [15] were used in the evaluation. However, for the

J-R curve properties, the values provided in Reference 11 for the SMAW weldments were compared with the lower bound curve provided in NUREG-6428 [16] for thermally aged welds. It was found that the lower bound curve in NUREG-6428 is more conservative and therefore was used in this evaluation. The properties used for the SMAW weldments are shown in Table 4-1.

The material properties shown in Table 4-1 are consistent with those recommended for use by the USNRC in its Safety Evaluation Report (SER) of the LBB application to portions of the Residual Heat Removal (RHR) at Ginna [4]. The materials of the RHR and the accumulator piping are similar and therefore the properties recommended by the USNRC for the RHR piping are equally applicable to the accumulator piping.

4.3 Piping Stresses

The piping stresses which are normally considered in a LBB evaluation are due to pressure, dead weight, thermal expansion and Safe Shutdown Earthquake (SSE). Summaries of the pipe stresses for the accumulator piping are shown in Table 4-2. These stresses are used to calculate the critical flaw size and the leakage rate through the 2.5 gpm leakage flaw size. For calculation of critical flaw size, the stress combination of pressure, deadweight, thermal and SSE loads is used. For leakage calculations, the stress combination of pressure, deadweight and thermal loads is used. These stress combinations are shown in Table 4-2 for the three nodal locations under consideration. These piping stresses are listed by their piping model node numbers, which are shown in Figures 1-1 and 1-2. These node numbers correspond to the weld locations along the piping system. Stress intensification factors based upon B31.1 piping Code for the accumulator piping [17] were calculated and used to determine the unintensified stresses based on the stresses obtained from the piping Stress Report [13]. This is justified because for the fracture mechanics evaluation, it is the stress in the weld which is of interest, and not that in the adjacent component. The modified stresses excluding stress intensification factors are also shown in Table 4-2. The moment stresses shown in these tables were conservatively calculated based on the extreme fiber.

Table 4-1

Material Properties for SMAW Weldment Used in LBB Evaluation

Parameter	Value
Temp (°F)	550
E (ksi)	25×10^3
$S_y = \sigma_o$ (ksi)	49.4
S_u (ksi)	61.4
Ramberg-Osgood Parameter α	9.0
Ramberg-Osgood Parameter n	9.80
J_{IC} (in-k/in^2)	0.288 (1)
J-R Curve Parameter C_1 (in-k/in^2)	3.816 (2)
J-R Curve Parameter N	0.643 (2)
J_{max} (in-k/in^2)	2.345 (3)

(1) A very conservative value of 40 kJ/m^2 = 0.228 in-kip/in^2 in Reference 16 was used.

(2) The J-R curve in Reference 16 was used and is given as

$$J_R = 40 + 83.5\,(\Delta a)^{0.643} \text{ kJ/m}^2$$
$$= 0.228 + 3.816\,(\Delta a)^{0.643} \text{ in-kip/in}^2$$

(3) Value of J_{max} was calculated at $\Delta a = 0.4$ inch.

Table 4-2

Calculation of Stresses for Accumulator Piping

Accumulator Piping														
		Input Intensified Stresses(ksi)[5]					*Unintensified Stresses(ksi)*						*Load Combination Stresses(ksi)*	
Location	Node	Type	P	DW	TH[1]	SSE	I	I*0.75[4]	P[2,7]	DW	TH[6]	SSE	P + DW + TH + SSE	P + DW + TH
Accumulator A	856	30° Taper Transition[8]	4.888	0.479	5.381	5.144	1.534	1.151	3.728	0.416	3.507	4.470	12.121	7.651
Accumulator B	60	Elbow[3]	4.927	0.146	2.242	6.617	1.111	0.834	3.728	0.146	2.017	6.617	12.508	5.891
	80	Elbow[3]	4.927	0.221	0.949	5.528	1.111	0.834	3.728	0.221	0.854	5.528	10.331	4.803

Notes:

1) Thermal Stress for Normal Operating Conditions.

2) Pressure Stress for Normal Operating Conditions (based upon pressure of 2235 psig): calculated with the following equation: (PDin^2)/(Dout^2-Din^2).

3) Stress Intensity factor I calculated for welding elbow with the following equation: I = 0.9/h^2/3 = 1.111 where h = TR/(t)^2 = 0.7286;

T = nominal wall thickness = 1.125 in., R = bend radius = 15 in., and r = mean radius = 4.8125 in.

4) I * 0.75 cannot be <1.

5) All input stresses taken from RGE-09Q-202.

6) Per B31.1, thermal stresses do not include 0.75 multiplier.

7) Per B31.1, pressure stresses do not include stress intensity factor, I.

8) Stress Intensity factor I, calculated for 30° taper transition with the following equation: I = 1.9 max or I = 1.3 + 0.0036D/t + 0.225/t

where D = outer diameter = 10.75 in. and t = thickness = 1.125 in.

5.0 LEAK-BEFORE-BREAK EVALUATION

The LBB approach involves the determination of critical flaw sizes, critical stresses and leakage through flaws. The critical flaw length for a through-wall flaw is that length for which, under a given set of applied stresses, the flaw would become marginally unstable. Similarly, the critical stress is that stress at which a given flaw size becomes marginally unstable. NUREG-1061, Vol. 3 [6] defines required margins of safety on both flaw length and applied stress. Both of these criteria will be examined in this evaluation. Circumferential flaws are more restrictive than postulated axial flaws because the critical flaw sizes for axial flaw are very long since they are affected by only pressure stress and result in large crack opening areas due to out of plane displacements. For this reason, the evaluation presented herein will be based on assumed circumferential flaws.

5.1 Evaluation of Critical Flaw Sizes

Critical flaw sizes may be determined using net section collapse criterion (NSCC) approach or J-Integral/Tearing Modulus (J/T) methodology. NSCC is particularly suited for materials with a considerable amount of ductility and toughness such as stainless steel materials, since it assumes that the cross-section of the pipe becomes fully plastic at the onset of failure. As such, for circumferential flaws, NSCC is less conservative compared to the J/T methodology which is based on elastic-plastic fracture mechanics (EPFM) principles. In this evaluation, the critical flaw sizes will therefore be determined based on the J/T approach.

A fracture mechanics analysis for determining the stability of through-wall circumferential flaws in cylindrical geometries such as pipes is presented in References 18 and 19. This procedure was used for the determination of critical stresses and flaw sizes in the accumulator piping at Ginna, using computer program, **pc-CRACK™** [20] which has been verified under SI's Quality Assurance program.

The expression for the J-integral for a through-wall circumferential crack under tension loading [18] which is applied in this analysis is:

$$J = f_1\left(a_e, \frac{R}{t}\right)\frac{P^2}{E} + \alpha\sigma_o\varepsilon_o c\left(\frac{a}{b}\right)h_1\left(\frac{a}{b}, n, \frac{R}{t}\right)\left[\frac{P}{P_o}\right]^{n+1}$$

where

$$f_1\left(a_e, \frac{R}{t}\right) = \frac{a_e F^2\left(\frac{a}{b}, \frac{R}{t}\right)}{4\pi R^2 t^2}$$

a_e	=	effective crack length including small scale yielding correction
R	=	mean pipe radius
t	=	pipe wall thickness
F	=	elasticity factor [18,19]
P	=	applied load = σ_∞ ($2\pi Rt$)
σ_∞	=	remote tension stress in the uncracked section
α	=	Ramberg-Osgood material coefficient
E	=	elastic modulus
σ_o	=	yield stress
ε_o	=	yield strain
2a	=	total crack length
2b	=	$2\pi R$
c	=	b-a
h_1	=	plasticity factor [18, 19]
P_o	=	limit load corresponding to a perfectly plastic material
n	=	Ramberg-Osgood strain hardening exponent.

Similarly, the expression for the J-integral for a through-wall crack under bending loading [19] is given by :

$$J = f_1\left(a_e, \frac{R}{t}\right)\frac{M^2}{E} + \alpha\sigma_o\varepsilon_o c\left(\frac{a}{b}\right)h_1\left(\frac{a}{b}, n, \frac{R}{t}\right)\left[\frac{M}{M_o}\right]^{n+1}$$

The parameters in the above equations are the same as the tension loading case except

M	=	applied moment = σ_∞ I/R
σ_∞	=	remote bending stress in the uncracked section
I	=	moment of inertia of the uncracked cylinder about the neutral axis
M_o	=	limit moment for a cracked pipe under pure bending corresponding to n = ∞ (elastic-perfectly plastic case)
	=	$M_o'\left[\mathrm{Cos}\left(\frac{\gamma}{2}\right) - \frac{1}{2}\mathrm{Sin}(\gamma)\right]$
M_o'	=	limit moment of the uncracked cylinder = $4\sigma_o R^2 t$

The Tearing Modulus (T) is defined by the expression:

$$T = \frac{dJ}{da}\frac{E}{\sigma_f^{\,2}}$$

Hence, in calculating T, J from the above expressions is determined as a function of crack size (a) and the slope of the J versus a curve is calculated in order to determine T. (The flow stress, σ_f, is taken as the mean of the yield and ultimate tensile strengths.) The material resistance J-R curve can also be transformed into J-T space in the same manner. The intersection of the applied and the material J-T curves is the point at which instability occurs and the crack size associated with this instability point is the critical crack size. This is shown schematically in Figure 5-1. An example of the critical flaw size determination for Node Point 60 under tension loading is shown in Figure 5-2.

The accumulator piping stresses consist of both tension and bending stresses. The tension stress is due to internal pressure while the bending stress is caused by deadweight, thermal and seismic loadings. Because a fracture mechanics model for combined tension and bending loading is not readily available, an alternate analysis is performed to determine the critical flaw length under such

loading condition using the tension and bending models separately. The stresses used in the fracture mechanics models are based on stresses calculated using the mean radius of the pipe. However, the extreme fiber stresses used in Section 4 are conservatively used. For the first case, the stress combination is assumed to be all due to tension and the critical flaw length is determined using the tension model. For the second case, the stress combination is assumed to be all due to bending and the critical flaw length is determined as such. The critical flaw sizes (lengths) obtained with the tension model (a_t) and the bending model (a_b) are combined to determine the actual critical flaw size (a_c) due to a combined tension and bending stress using linear interpolation, as described by the following equation:

$$a_c = a_t \frac{\sigma_t}{\sigma_b + \sigma_t} + a_b \frac{\sigma_b}{\sigma_b + \sigma_t}$$

where σ_t and σ_b are the piping tensile and bending stresses respectively.

The results of the critical flaw length determination are presented in Tables 5-1 and 5-2. In Table 5-1, the half critical flaw length is determined for the normal + SSE stress combination. The leakage flaw total length in this case must be less than the half critical flaw length (a_c). In Table 5-2, the critical flaw length is determined with a factor of $\sqrt{2}$ on the normal + SSE stresses. The leakage flaw length in this case must be less than the total flaw length ($2a_c$). The final leakage flaw length must be less than the minimum of these two cases. This final leakage flaw length is used in calculating leakage in the next section. In comparison of Tables 5-1 and 5-2, it can be seen that the limiting critical flaw size is based on a factor of unity on the stresses (Table 5-1).

5.2 Leak Rate Determination

Calculations were performed to determine the flaw sizes that would result in 2.5 gpm leakage. The calculations were performed using the PICEP computer program developed by EPRI [21, 22]. The flow rate equations in PICEP are based on Henry's homogeneous nonequlibrium critical flow model [23]. The program accounts for nonequlibrium "flashing" mass transfer between liquid and vapor phases, fluid friction due to surface roughness and convergent flow paths.

In the determination of leak rates using PICEP, the following assumptions are made:

- A plastic zone correction is included. This is consistent with fracture mechanics principles for ductile materials.
- The crack is assumed to be elliptical in shape. This is the most reasonable assumption those available in PICEP.
- Crack roughness is taken as 0.000197 inches [22].
- There are no turning losses assumed since the crack is assume to be initiated by some mechanism other than IGSCC.
- A sharp-edged entrance loss factor of 0.61 is used (PICEP default).
- The default friction factors of PICEP are utilized.
- The crack length is constant through the thickness.
- The load combination used is pressure, dead weight and thermal expansion stresses.

The leakage flaw size was evaluated for normal operating conditions for an operating pressure of 2250 psia (2235 psig) and a temperature of 550°F using location-unique stresses in Table 4-2 and material properties shown in Table 4-1. Table 5-3 shows the predicted leakage flaw sizes to produce 2.5 gpm leakage at each location.

5.3 LBB Evaluation Results and Discussions

Table 5-4 provides a comparison between the critical flaw size and the flaw size that produces 2.5 gpm leakage at the weld locations. It can be seen that in all cases, the one-half critical flaw size based on normal + SSE loads is greater that the 2.5 gpm leakage size flaw, thus satisfying the factor of two on flaw size required by NUREG-1061, Volume 3. Flaw size margin was also evaluated using $\sqrt{2}$ times normal plus SSE loads, and greater margins on flaw size was demonstrated at the three nodal locations.

Table 5-1

Half Critical Flaw Length (Normal + SSE Stresses)

	Node	Stresses (ksi)		Half Critical Length (in)		
		Bending (σ_b)	Tension (σ_t)	Bending (a_b)	Tension (a_t)	Combined (a_c)
Accumulator A Piping	856	8.393	3.728	7.3582	6.3554	7.0498
Accumulator B Piping	60	8.780	3.728	7.2547	6.2418	6.9528
	80	6.603	3.728	7.559	6.9267	7.3308

Table 5-2

Critical Flaw Sizes (Factor of $\sqrt{2}$ on Normal + SSE Stresses)

	Node	Stresses (ksi)		Critical Length (in)		
		Bending (σ_b)	Tension (σ_t)	Bending ($2a_b$)	Tension ($2a_t$)	Combined ($2a_c$)
Accumulator A Piping	856	11.869	5.272	12.2684	10.1208	11.6078
Accumulator B Piping	60	12.417	5.272	12.0288	9.8772	11.3876
	80	9.338	5.272	13.4456	11.3394	12.6856

Table 5-3

Predicted Leakage Rates for Normal Operating Stresses

	Node	2.5 gpm Leakage Flaw Size (2a) (in.)	Crack Opening Area (in.)
Accumulator A Piping	856	4.103	0.00931
Accumulator B Piping	60	4.637	0.00972
	80	5.074	0.01004

Table 5-4

Comparison of Critical and 2.5 gpm Leakage Flaws

	Node	One-Half Critical Flaw Size (in.)	2.5 gpm Leakage Flaw Size (in.)
Accumulator A Piping	856	7.0498	4.103
Accumulator B Piping	60	6.9528	4.637
	80	7.3308	5.074

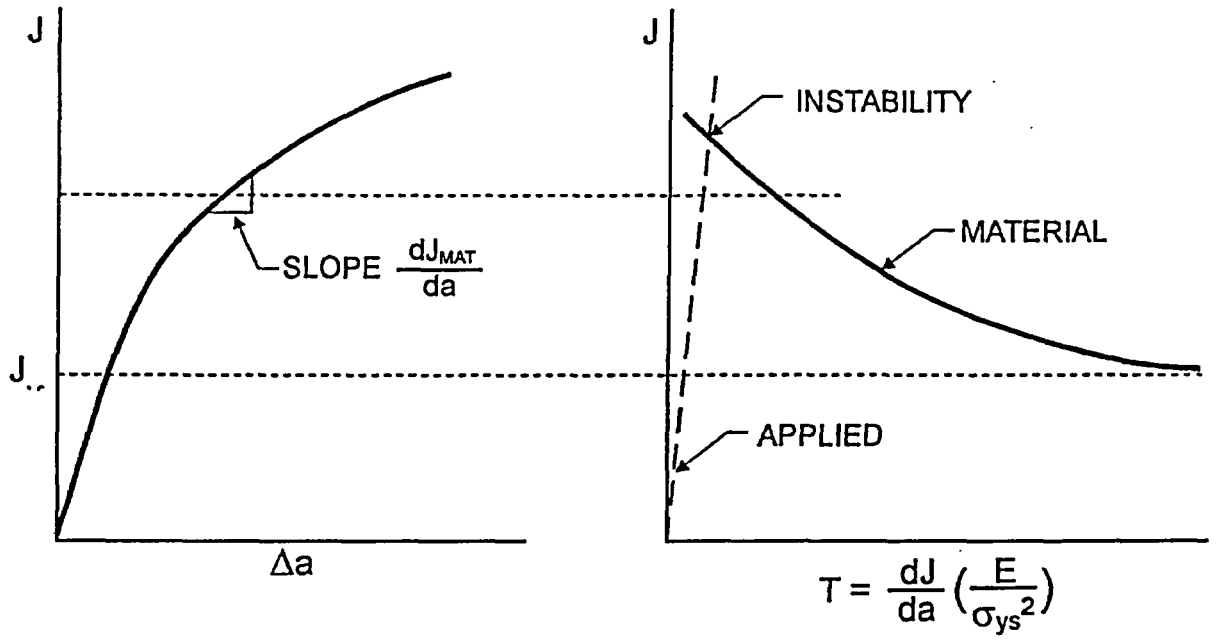

93220r0

Figure 5-1. J-Integral/Tearing Modulus Concept for Determination of Instability During Ductile Tearing

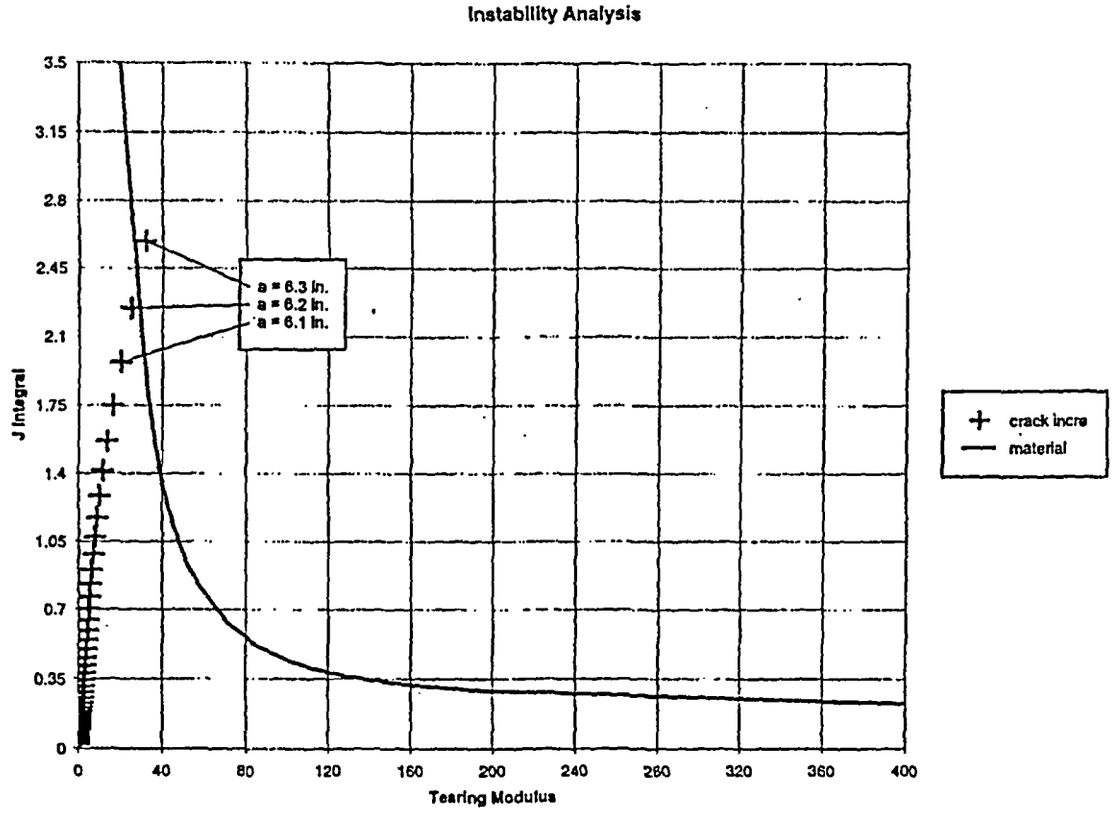

Figure 5-2. Determination of Critical Flaw Size Under Tension Loading for Node 60 Using J-T Approach

6.0 EVALUATION OF FATIGUE CRACK GROWTH OF SURFACE FLAWS

In accordance with the NRC criteria [5,6] set forth in Section 2 of this report, the growth of postulated surface cracks by fatigue is evaluated to demonstrate that such growth is insignificant for the plant life, when initial flaw sizes in excess of those meeting ASME Code Section XI, IWB-3514 are postulated. Furthermore, the growth of larger postulated initial flaws, in both depth and length directions, is studied to demonstrate that such flaws would tend to grow through the pipe wall (in the depth direction) to result in detectable leakage prior to significantly impacting safety margins by extending in length.

Plant design transients for the accumulator piping [24,25] are shown in Table 6-1. For the purpose of crack growth analysis, the transients shown in Table 6-1 are conservatively combined into fourteen (14) different load combinations based on their pressure and temperature ranges. The combined transients and associated number of cycles are shown in Table 6-2. The pressure and temperature values corresponding to these combined transients were used to linearly scale the pressure and thermal stresses corresponding to operating conditions. The axial stresses due to the pressure and thermal differentials for each of the transient categories are calculated as follows:

For a change in pressure of ΔP, the axial stress is calculated as:

$$\sigma_p = \Delta P \frac{D_i^2}{D_o^2 - D_i^2}$$

where D_o is the outside diameter and D_i is the inside diameter.

For thermal loads, ΔT, the stress is the maximum operating thermal stress, shown in Table 4-2, factored by the ratio of the transient temperature to the operating temperature gradients:

$$\sigma_t = \sigma_{max,oper} \frac{\Delta T}{\Delta T_{oper}}$$

The calculated axial pressure and thermal stresses are presented in Table 6-3. Table 6-3 also shows the total stresses, including the maximum dead weight stress for Nodes 60, 80, and 856, which is shown in Table 4-2. The maximum intensified dead weight stress from Table 4-2 is conservatively used in this evaluation.

The stress intensity factors, K, corresponding to the point of the maximum depth of a semi-elliptical crack are calculated using **pc-CRACK™** [20]. The K values are calculated for each pipe size for a reference 1 ksi uniform tension and pure bending stress. In each case, the stress intensity factors are determined for a conservative aspect ratio (a/ℓ) of 0.1. The stress intensity magnification factors derived in Reference 26 were used to compute the K value corresponding to the point of maximum length at the inside surface of the pipe.

Using the K results calculated with **pc-CRACK™** [20] and the transients in Table 6-2, the fatigue crack growth law recommended in Reference 15 for stainless steel in a PWR environment was employed to compute crack growth for various postulated initial flaw sizes. This crack growth is given by:

$$da/dN = C\,E\,S\,(\Delta K)^n$$

where

da/dN	=	change in crack depth, a, per fatigue cycle, in./cycle
C, n	=	material constants, n = 3.3, C = 2×10^{-19} (in./cycle)/(psi$\sqrt{\text{in}}$)^n
S	=	R ratio correction factor = $[1.0 - 0.5R^2]^{-4}$
R	=	K_{min}/K_{max}
E	=	environmental factor (equal to 1.0, 2.0, and 10.0 for air, PWR, and BWR environments, respectively)
ΔK	=	$K_{max} - K_{min}$, psi$\sqrt{\text{in}}$ and
K_{min}, K_{max}	=	minimum and maximum values, respectively, of applied stress intensity factor

A value of 2.0 was used for the parameter E in the above equation. Two bounding R ratios of 0.0 and 1.0 were used to calculate the crack growth. The R ratio of 0.0 corresponds to a case where the

effect of residual stresses is minimal while an R ratio of 1.0 conservatively represents the case where residual stresses contribute significantly to the total stresses. In equivalent ksi units, the crack growth laws for these two R ratios can be written as:

$$da/dN = 3.177 \times 10^{-9} (\Delta K)^{3.3} \text{ for } R = 0.0$$

$$da/dN = 5.083 \times 10^{-8} (\Delta K)^{3.3} \text{ for } R = 1.0$$

The analysis is performed for Node point 856 of the Accumulator A piping since this location has the maximum thermal stress range and maximum dead weight stress as can be seen from Table 4-2. The stresses are cycled between the maximum and minimum stresses shown in Table 6-3. The weld residual stress is conservatively represented by a pure through-wall bending stress equal to the pipe material (SA 376, Type 316 stainless steel) yield stress at the operating temperature of 612.2°F (S_y = 18.8 ksi). For each pipe size and enveloping transient category, the appropriate scaling factors, based upon a reference stress of 1 ksi and actual stress values given in Table 6-3, are input to obtain the actual K values for the fatigue crack growth.

For the crack growth in the depth direction, the analysis is performed for three initial crack depths (a/t=0.15, 0.5 and 0.7). In the length direction, the calculations are performed for depth-to-wall thickness ratios (a/t) = 0.20, 0.6 and 0.8. These ratios correspond approximately to the final a/t ratios for crack growth in the depth direction after 40 years or when the crack reaches 80% of pipe thickness.

The fatigue crack growth analysis results are summarized in Table 6-4. It can be seen that postulated circumferential flaws 15% of pipe wall by about 1.69 inches long (ℓ/a = 10) do not grow significantly in 40 years of plant operation. Evaluation of deeper postulated flaws (50% and greater) for both R ratios, shows that such cracks would grow through the pipe wall before extending significantly in length. In all cases, the crack would grow through-wall before extending in length more than 0.12 inches. Thus, detectable leakage would result before LBB safety margins are violated.

Table 6-1

Plant Design Transients for Accumulator Piping

Design Condition	Design Transients	Number of Cycles	$\Delta P^{(1)}$ (psi)	$\Delta T^{(1)}$ (°F)
Level A	Plant Heatup/Cooldown	200	2250	477
	Plant Loading/Unloading	14,500	0	5
	10% Step Increase/Decrease	2,000	180	29
	Steady State Fluctuations	Infinite	100	6
Level B	Reactor Trip at Full Power	400	320	23
	Step Reduction 50% to 0%	400	100	16
	Loss of Power	40	950	53
	Loss of Load	80	1250	53
	Loss of Flow	80	340	37
Test	Primary Pressure Test	40	2485	300
	Primary Leakage Test	100	2250	200

(1) Maximum ΔP and ΔT assumed.

Table 6-2

Combined Transients For Fatigue Crack Growth Evaluation
for Accumulator Piping

Load Case	Load Combination Description	Block Cycles[3]	P_{max} psig	P_{min} psig	T_{max} °F	T_{min} °F	ΔP, psi	ΔT, °F	Notes
1	Pressure Test	1	2485	0	547	70	2485	477	Max ΔT assumed
2	Leak Test	2.5[1]	2250	0	547	70	2250	477	Max ΔT assumed
3	Heatup/Cooldown + Loss of Load (Up)	2	2800	0	600	70	2800	530	
4	Heatup/Cooldown + Loss of Power (Up)	1	2500	0	600	70	2500	530	
5	Heatup/Cooldown + 50% Reduction (Up)	2	2350	0	562	70	2350	492	
6	50% Reduction (Up) + Loss of Power (Dn)	1	2350	1550	562	547	800	15	
7	50% Reduction (Up) + Loss of Load (Dn)	2	2350	1550	562	547	800	15	
8	50% Reduction (Up) + Loss of Flow (Dn)	2	2350	1910	562	520	440	42	
9	50% Reduction (Up) + Reactor Trip (Dn)	3	2350	1930	562	547	420	15	
10	10% Step Increase (Up) + Reactor Trip (Dn)	7	2330	1930	568	547	400	21	
11	10% Step Incr(Up) + 10% Step Decr (Dn)	43	2330	2150	568	539	180	29	
12	10% Step Decr (Up) + 10% Step Decr (Dn)	7	2290	2150	555	539	140	16	
13	10% Step Decr (Up) + 10% Step Incr (Dn)	43	2290	2150	555	551	140	4	
14	Remaining (Up) + Remaining (Dn)	369.5[2]	2250	2150	557	547	100	10	

(1) For analysis purposes, 3 cycles are used.
(2) For analysis purposes, 378 cycles are used.
(3) Numbers in block are for 1/40th of plant life. 40 blocks of cycles used in analysis.

Table 6-3

Combined Maximum and Minimum Stresses for Fatigue Growth Analysis for Accumulator Piping

Load Combination	Maximum Stress, ksi				Minimum Stress, ksi			
	P	Th	DW	Total	P	Th	DW	Total
1	4.145	3.085	0.479	7.710	0.000	0.000	0.479	0.479
2	3.753	3.085	0.479	7.318	0.000	0.000	0.479	0.479
3	4.671	3.428	0.479	8.578	0.000	0.000	0.479	0.479
4	4.170	3.428	0.479	8.077	0.000	0.000	0.479	0.479
5	3.920	3.312	0.479	7.711	0.000	0.000	0.479	0.479
6	3.920	3.312	0.479	7.711	2.586	3.085	0.479	6.150
7	3.920	3.312	0.479	7.711	2.586	3.085	0.479	6.150
8	3.920	3.312	0.479	7.711	3.186	2.911	0.479	6.576
9	3.920	3.312	0.479	7.711	3.219	3.085	0.479	6.784
10	3.887	3.221	0.479	7.587	3.219	3.085	0.479	6.784
11	3.887	3.221	0.479	7.587	3.586	3.034	0.479	7.099
12	3.820	3.137	0.479	7.436	3.586	3.034	0.479	7.099
13	3.820	3.137	0.479	7.436	3.586	3.111	0.479	7.177
14	3.753	3.150	0.479	7.382	3.586	3.085	0.479	7.151

(1) A through-wall bending weld residual stress equal to the yield stress was also applied.

Table 6-4

Results of Fatigue Crack Growth

R ratio	Assumed Initial a/t	Assumed Initial Depth (in.)	Final Depth (in.)	Final a/t	Assumed Initial Length (in.)	Final Length (in.)	Change in Length (in.)
0.0	0.15	0.1688	0.1691	15%	1.125	1.125	0.000
	0.50	0.5625	0.5698	51%	3.375	3.377	0.002
	0.70	0.7875	0.8077	72%	4.500	4.507	0.007
1.0	0.15	0.1688	0.1752	16%	1.125	1.126	0.001
	0.50	0.5625	0.7313	65%	3.375	3.410	0.035
	0.70	0.7875	0.9000	80%	4.500	4.618	0.118

7.0 SUMMARY AND CONCLUSIONS

Leak-before-break (LBB) evaluations are performed for portions of the Accumulator A and B piping at Ginna in accordance with the requirements of NUREG-1061. The analysis was performed using conservative generic material properties for the base metals and weldments. Location specific stresses consisting of pressure, deadweight, thermal and seismic loads were used in the analysis. In the evaluations, circumferential flaws are considered since they are more limiting than axial flaws. Critical flaw sizes and leakage flaw sizes were calculated on a location specific basis for the pressurizer surge line for several material conditions. Conservative weld metals properties were used in the evaluation. The effect of thermal embrittlement was considered for the SMAW weld metal. The minimum of one half the critical flaw size with a factor of one on the stresses or the full critical flaw size with a factor of $\sqrt{2}$ on the stresses were determined and were compared to the crack sizes that would produce 2.5 gpm leakage. Fatigue crack growth analysis was also performed to determine the extent of growth of any pre-existing flaws.

Based on these evaluations, the following conclusions can be made.

- The detectable leakage at Ginna is 0.25 gpm. Based on the required margin of 10 on leakage in NUREG-1061, Volume 3, the critical flaw sizes were compared to the crack size which produces 2.5 gpm leakage. The critical flaw sizes, based on the NUREG-1061, Vol. 3 margins, were found to be significantly greater than the 2.5 gpm leakage flaw sizes at all locations, thus assuring leak-before-break.

- Fatigue crack growth of hypothetical 10:1 surface flaw with initial depth of 15% of pipe wall was found to be insignificant for the expected number of heatup and cooldown cycles over the plant lifetime. Therefore fatigue does not invalidate the application of leak-before-break evaluation to the accumulator piping.

- The effects of other degradation mechanisms which could invalidate the LBB evaluations were considered in the evaluation. It was determined that there is no potential for water hammer,

intergranular stress corrosion cracking (IGSCC) and flaw-assisted corrosion for the accumulator piping at Ginna

8.0 REFERENCES

1. Rochester Gas & Electric Corporation Drawings:

   a) C-381-354 Sheet 3
   b) C-381-355 Sheet 8
   c) C-381-355 Sheet 7

2. Structural Integrity Associates Report No. SIR-97-077, Rev. 0, "Leak-Before-Break Evaluation of Portions of the Residual Heat Removal (RHR) System at R. E. Ginna Nuclear Power Station."

3. Structural Integrity Associates Report No. SIR-98-071, Rev. 1, "Responses to U.S. NRC Request for Additional Information Regarding Request for Leak-Before-Break Approval of Portions of the R. E. Ginna Nuclear Power Plant Residual Heat Removal System Piping (TAC # MAC-389)."

4. Letter from G. S. Vissing (USNRC) to R. C. Mecredy (RG&E) including Safety Evaluation Report, "Staff Review of the Submittal by Rochester Gas and Electric Company to Apply Leak-Before-Break Status to Portions of the R. E. Ginna Nuclear Power Plant Residual Heat Removal System Piping (TAC No. MA039)," dated February 25, 1999, *Docket No. 50-244.*

5. Stello, Jr., V., "Final Broad Scope Rule to Modify General Design Criterion 4 of Appendix A, 10 CFR Part 50", NRC SECY-87-213, Rulemaking Issue (Affirmation), August 21, 1987.

6. NUREG-1061, Volumes 1-5, "Report of the U. S. Nuclear Regulatory Commission Piping Review Committee", prepared by the Piping Review Committee, NRC, April 1985.

7. NUREG-0927, "Evaluation of Water Hammer Occurrence in Nuclear Power Plants" *Revision 1.*

8. EPRI Report, TR-106438, 2856-02, "Water Hammer Handbook For Nuclear Plant Engineers And Operators", May 1996.

9. RG&E Action Reports 97-0404 & 0405.

10. W. S. Hazelton, W. H. Koo, "Technical Report on Material Selection and Processing Guidelines for BWR Coolant pressure Boundary Piping", NUREG-0313, Rev. 2, USNRC, January 1988.

11. EPRI Report NP-3944, "Erosion-Corrosion in Nuclear Plant Steam Piping: Cause and Inspection Program Guidelines," April 1985.

12. Bechtel Corporation, Weld Standard, Procedure Specification P8-AT-g ("Y" Type Insert Ring), Rev. 0, March 22, 1967; P8-AT-g, Rev. 3, February 23, 1967.

13. Westinghouse Stress Report, SDTAR-80-05-26, SI-200 dated 3/20/81.

14. EPRI Report No. NP-6301-D "Ductile Fracture Handbook", June 1989.

15. ASME Section XI Task Group for Piping Flaw Evaluation, ASME Code, "Evaluation of Flaws in Austenitic Steel Piping," Journal of Pressure Vessel Technology, Vol. 108, August 1986, pp. 352-366.

16. NUREG/CR-6428, "Effects of Thermal Aging on Fracture Toughness and Charpy-Impact Strength of Stainless Steel Pipe Welds," May 1996.

17. American National Standard, Power Piping, ANSI B31.1, 1973 Edition with Summer Addenda.

18. Kumar, V., et al., "Advances in Elastic-Plastic Fracture Analysis," EPRI NP-3607, August 1984.

19. Kumar, V., et al., "An Engineering Approach for Elastic-Plastic Fracture Analysis," EPRI NP-1931, July 1981.

20. Structural Integrity Associates, Inc., "**pc-CRACK™** Fracture Mechanics Software", Version 3.1 – 98348, 1999.

21. EPRI Report NP-3596-SR, "PICEP: Pipe Crack Evaluation Computer Program," Rev. 1, July 1987.

22. EPRI Report NP-3395, "Calculation of Leak Rates Through Crack in Pipes and Tubes," December 1983.

23. P.E. Henry, "The two-Phase Critical Discharge of Initially Saturated or Subcooled Liquid," Nuclear Science and Engineering, Vol. 41, 1970.

24. Ginna UFSAR, Table 5/1-4, Rev. 13 dated 12/96.

25. BWI Report No. 222-7705-SR-2, "Transient Analysis of Tubesheet/Primary Head and Secondary Shell Assembly," Section 2.1, October 2, 1995.

26. W. Huget and K. Esser, "Stress Intensity Factors for Slender Surface Cracks," SMiRT Conference, Paper G/F 3/4, Chicago, 1983.